International Journal of Current Trends in Engineering & Technology
ISSN: 2395-3152
Volume: 12, Issue: 05 (September-October, 2026)

Deep Learning-Based Successive Interference Cancellation for Non-Orthogonal Multiple Access in 5G Wireless Networks

Teklal Mahto [1], Ankush Shrivastava [2],
[1,2] Department of Computer Science and Engineering, RKDF University, Bhopal, India
[1]teklalkumarmahto@gmail.com, [2]ankushshrivastava19@gmail.com,

Abstract

This research proposes a hybrid deep learning-based Successive Interference Cancellation (SIC) framework using Long Short-Term Memory (LSTM) and Convolutional Neural Networks (CNN) to improve interference management in 5G wireless communication systems, particularly in Non-Orthogonal Multiple Access (NOMA) networks. The proposed CNN-LSTM architecture combines the ability of CNN to extract spatial features and local signal patterns with the capability of LSTM to capture temporal dependencies in wireless signals. Unlike conventional SIC methods, which basically rely on perfect Channel State Information (CSI) and fixed decoding orders, the proposed framework predicts the optimal interference cancellation order and estimates residual interference. This helps minimize error propagation and improve signal detection reliability under varying channel conditions. The proposed framework is evaluated through simulations involving different signal-to-noise ratios (SNRs) and user densities. The results demonstrate improved interference cancellation accuracy, reduced Bit Error Rate (BER), and enhanced overall system performance compared with conventional SIC and standalone deep learning approaches.

Keywords: 5G Wireless Networks, Successive Interference Cancellation (SIC), Deep Learning, Long Short-Term Memory (LSTM), Convolutional Neural Network (CNN), Interference Management, Bit Error Rate (BER), Signal Processing, Hybrid Neural Networks

1 Introduction

The widespread adoption of smartphones, Internet of Things (IoT) devices, and emerging technologies such as augmented reality, autonomous driving, and ultra-high-definition video streaming has led to an exponential increase in wireless data traffic. Consequently, future wireless communication networks face growing demands for improved spectral efficiency and massive user connectivity [1]. Fifth-generation (5G) and beyond-fifth-generation (B5G) networks are expected to support diverse applications with distinct Quality of Service (QoS) requirements, including enhanced Mobile Broadband (eMBB), Ultra-Reliable Low-Latency Communications (URLLC), and massive Machine-Type Communications (mMTC). To address these requirements, Non-Orthogonal Multiple Access (NOMA) has gained considerable attention as an advanced multiple-access technique that enables more efficient utilization of radio resources [2, 3].

Unlike conventional Orthogonal Multiple Access (OMA), which assigns separate time, frequency, or code resources to individual users, NOMA allows multiple users to transmit simultaneously over the same resource block through power-domain or code-domain multiplexing [4, 5]. This approach improves spectral efficiency, increases network connectivity, and offers better user fairness. At the receiver, Successive Interference Cancellation (SIC) is commonly adopted to recover individual user signals from the superimposed transmission. The decoding process generally follows the users' channel conditions, allowing interference to be sequentially estimated and removed to facilitate reliable signal detection [6].

Although SIC provides significant performance benefits, its conventional implementation encounters several challenges in practical wireless environments:

- **Error Propagation:** Incorrect detection of an interfering signal of the user can introduce errors into subsequent cancellation stages, which results in reduced detection accuracy and degraded system performance [7].
- **Imperfect Channel State Information (CSI):** Conventional SIC depends on accurate channel estimates. However, pilot contamination, feedback delays, and channel variations can introduce estimation errors, which leads to incomplete interference cancellation and reduced detection reliability [8].
- **Nonlinear Channel Impairments:** Traditional linear detection techniques may not adequately capture complex interference characteristics and nonlinear channel effects, particularly under high mobility and frequency-selective fading conditions [9].

- **Processing Latency:** The sequential decoding mechanism increases computational complexity and processing time with the number of users, which finally makes conventional SIC challenging for latency-sensitive applications such as URLLC [9, 10].

To overcome these limitations, Deep Learning (DL) has attracted increasing interest as an alternative approach to solving complex physical-layer challenges in wireless communication systems [11]. Deep neural networks can automatically learn complex signal characteristics, approximate nonlinear relationships, and adapt to changing channel conditions without requiring explicit mathematical descriptions of the underlying communication environment. These capabilities make DL particularly suitable for interference management and signal detection in NOMA systems
citeBanerjee. Initial research on DL-assisted NOMA primarily investigated replacing conventional signal processing components, including channel estimation and symbol detection, with neural network-based solutions [12]. These developments demonstrated improved detection performance, especially under imperfect CSI and nonlinear channel conditions [13].

Subsequently, several deep learning architectures have been investigated to enhance signal detection in NOMA systems. Convolutional Neural Networks (CNNs) have demonstrated their effectiveness in extracting spatial characteristics and local features from received signal representations. By learning hierarchical feature patterns, CNNs can identify complex multi-user interference structures and channel correlations [14]. Nevertheless, conventional CNN architectures have limited capability to capture long-term temporal dependencies associated with time-varying fading channels and user mobility [15].

In contrast, Long Short-Term Memory (LSTM) networks, a specialized form of Recurrent Neural Networks (RNNs), are designed to learn temporal relationships in sequential data [16]. Their application in wireless communication enables the modeling of dynamic channel variations, tracking of user mobility, and prediction of channel behavior over time. These characteristics make LSTM networks particularly effective for dynamic NOMA environments [17]. Furthermore, their internal memory cells and gating mechanisms facilitate the learning of long-term dependencies while alleviating the vanishing gradient problem commonly encountered in conventional RNN architectures.

2 Related Work

This section provides an overview of the existing literature on Successive Interference Cancellation (SIC), massive Non-Orthogonal Multiple Access (NOMA), and their associated integrated technologies. It also identifies the major research limitations and open challenges that establish the motivation for the proposed study.

NOMA has emerged as a promising multiple-access technology for fifth-generation (5G) wireless communication systems, primarily due to its ability to support multiple users within the same radio resource block through power-domain multiplexing. Saito *et al.* [18] introduced the fundamental concept of NOMA and demonstrated its advantages over Orthogonal Multiple Access (OMA) in terms of achievable sum rate and user fairness. Ding *et al.* [19] presented an extensive review of NOMA, covering essential aspects such as power allocation, user pairing, and cooperative communication. Similarly, Islam *et al.* [20] investigated the role of SIC in enabling NOMA and reviewed significant developments in NOMA-based 5G networks, including capacity analysis, power allocation strategies, user fairness, and user-pairing mechanisms. Furthermore, the integration of NOMA with advanced communication technologies, including Multiple-Input Multiple-Output (MIMO) and millimeter-wave communications, was investigated in [21], with particular emphasis on the influence of user pairing on overall system performance.

Shi and Ouyang [22] investigated a NOMA-assisted Mobile Edge Computing (MEC) framework in which multiple devices simultaneously offload computational tasks to different edge servers to minimize execution latency. They developed an optimization-based resource allocation strategy that reduced both processing delays and operational costs compared with conventional approaches. The proposed framework also demonstrated its applicability to multi-device Internet of Things (IoT) environments. In another study, Benjebbour *et al.* [23] examined NOMA as a downlink multiple-access approach for Long-Term Evolution (LTE) and 5G networks. Their investigation highlighted the advantages of NOMA over conventional Orthogonal Frequency Division Multiple Access (OFDMA), including its compatibility with MIMO technology. Simulation and experimental evaluations reported performance improvements exceeding 30% at both link and system levels compared with OFDMA.

Recently, the application of Deep Learning (DL) techniques to improve SIC performance in NOMA systems has received considerable research attention. Farsad *et al.* [12] proposed SICNet, a deep neural network (DNN)-based framework that replaces conventional SIC processing blocks with trainable neural network layers. This approach demonstrated the potential of data-driven learning for improving signal detection and interference cancellation. Chuan *et al.* [24] investigated the application of Convolutional Neural Networks (CNNs) to uplink NOMA signal detection. Their study demonstrated that CNN-based detection methods can recover the information transmitted by multiple users simultaneously, reducing dependence on conventional communication signal processing algorithms.

International Journal of Current Trends in Engineering & Technology
ISSN: 2395-3152
Volume: 12, Issue: 05 (September-October, 2026)

3 System Model

3.1 Downlink NOMA System Model

Consider a downlink NOMA system with one base station (BS) which serves K users over a shared frequency band. The BS transmits a superimposed signal to all users simultaneously. Let $x_k(t)$ denote the transmitted symbol for user k at time instant t, with $\mathbb{E}[|x_k(t)|^2] = 1$. The power allocation coefficient for user k is denoted by $\sqrt{P_k}$, which satisfies the total power constraint $\sum_{k=1}^{K} P_k \leq P_{total}$, where P_{total} is the total transmit power.

The superimposed transmitted signal at time t is expressed as:

$$s(t) = \sum_{k=1}^{K} \sqrt{P_k} x_k(t) \tag{1}$$

The received signal at user k is given by:

$$y_k(t) = h_k(t)s(t) + n_k(t) \tag{2}$$

where $h_k(t)$ represents the complex channel coefficient between the BS and user k, and $n_k(t) \sim \mathcal{CN}(0, \sigma_k^2)$ is the additive white Gaussian noise (AWGN) at user k.

3.2 Channel Model

The channel coefficient $h_k(t)$ incorporates both large-scale fading and small-scale fading effects:

$$h_k(t) = \sqrt{\beta_k(t)} \cdot g_k(t) \tag{3}$$

where $\beta_k(t)$ represents the large-scale fading (path loss and shadowing) given by:

$$\beta_k(t) = \frac{G \cdot L}{(d_k)^{\alpha} \cdot \psi_k(t)} \tag{4}$$

Here, G is the antenna gain, L is the system loss factor, d_k is the distance from BS to user k, α is the path loss exponent, and $\psi_k(t)$ represents shadowing effects modeled as a log-normal random variable. The small-scale fading coefficient $g_k(t)$ follows a Rayleigh distribution with $\mathbb{E}[|g_k(t)|^2] = 1$.

3.3 Conventional SIC Receiver

In conventional SIC, the users are ordered based on their channel gains. Assuming $|h_1|^2 \geq |h_2|^2 \geq \cdots \geq |h_K|^2$, the user with the strongest channel gain (user 1) decodes its signal last after canceling interference from all other users.

The signal-to-interference-plus-noise ratio (SINR) for the user k when decoding user j's signal ($j \leq k$) is:

$$\text{SINR}_{j \to k} = \frac{P_j |h_k|^2}{\sum_{i=j+1}^{K} P_i |h_k|^2 + \sigma_k^2} \tag{5}$$

The achievable rate for the user k is:

$$R_k = \log_2 \left(1 + \frac{P_k |h_k|^2}{\sum_{i=k+1}^{K} P_i |h_k|^2 + \sigma_k^2} \right) \tag{6}$$

3.4 Problem Formulation

The conventional SIC suffers from error propagation and imperfect channel estimation. The received signal after imperfect SIC can be modeled as:

$$\tilde{y}_k(t) = \underbrace{\sqrt{P_k} h_k(t) x_k(t)}_{\text{desired signal}} + \underbrace{\sum_{i=k+1}^{K} \sqrt{P_i} h_k(t) \hat{x}_i(t)}_{\text{residual interference}} + \underbrace{\sum_{j=1}^{k-1} \sqrt{P_j} h_k(t) \Delta x_j(t)}_{\text{error propagation}} + n_k(t) \tag{7}$$

where $\hat{x}_i(t)$ is the estimated symbol and $\Delta x_j(t) = x_j(t) - \hat{x}_j(t)$ represents the estimation error.

4 Proposed Methodology

4.1 Overall Architecture

The proposed LSTM-CNN-based Advanced SIC (LSTM-CNN-ASIC) framework consists of three main components: channel estimation module, signal detection module, and interference cancellation module. The overall architecture is illustrated in Figure 1.

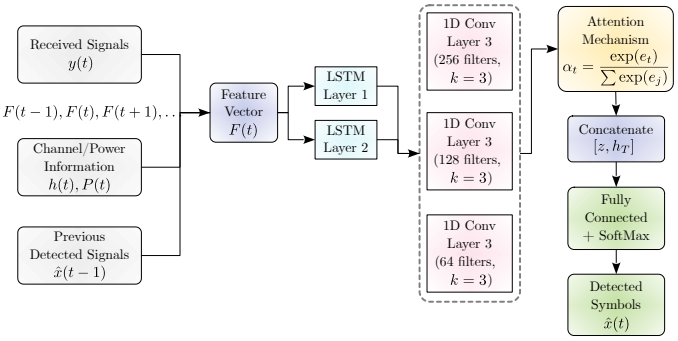


Fig. 1: Proposed LSTM-CNN-ASIC Architecture

4.2 Input Feature Representation

The input to the LSTM-CNN network at time t is a multi-dimensional feature vector constructed from the received signal and channel state information:

$$\mathbf{F}(t) = [\mathbf{y}(t), \mathbf{h}(t), \mathbf{P}(t), \hat{\mathbf{x}}(t-1)] \tag{8}$$

where
$\mathbf{y}(t) = [y_1(t), y_2(t), \ldots, y_K(t)]^T$ is the received signal vector,
$\mathbf{h}(t) = [h_1(t), h_2(t), \ldots, h_K(t)]^T$ is the channel coefficient vector,
$\mathbf{P}(t) = [P_1(t), P_2(t), \ldots, P_K(t)]^T$ is the power allocation vector, and
$\hat{\mathbf{x}}(t-1)$ represents previously detected symbols.

4.3 LSTM for Temporal Feature Extraction

The LSTM network captures temporal dependencies in the received signal sequence. The LSTM cell state and hidden state updates are given by:

$$\mathbf{i}_t = \sigma(\mathbf{W}_i \mathbf{F}(t) + \mathbf{U}_i \mathbf{h}_{t-1} + \mathbf{b}_i) \quad (9)$$
$$\mathbf{f}_t = \sigma(\mathbf{W}_f \mathbf{F}(t) + \mathbf{U}_f \mathbf{h}_{t-1} + \mathbf{b}_f) \quad (10)$$
$$\mathbf{o}_t = \sigma(\mathbf{W}_o \mathbf{F}(t) + \mathbf{U}_o \mathbf{h}_{t-1} + \mathbf{b}_o) \quad (11)$$
$$\mathbf{c}_t = \mathbf{f}_t \odot \mathbf{c}_{t-1} + \mathbf{i}_t \odot \tanh(\mathbf{W}_c \mathbf{F}(t) + \mathbf{U}_c \mathbf{h}_{t-1} + \mathbf{b}_c) \quad (12)$$
$$\mathbf{h}_t = \mathbf{o}_t \odot \tanh(\mathbf{c}_t) \quad (13)$$

where $\mathbf{i}_t$, $\mathbf{f}_t$, $\mathbf{o}_t$ are the input, forget, and output gates respectively, $\mathbf{c}_t$ is the cell state, $\mathbf{h}_t$ is the hidden state, $\sigma(\cdot)$ is the sigmoid function, and $\odot$ denotes element-wise multiplication.

4.4 CNN for Spatial Feature Extraction

The output of the LSTM layer $\mathbf{H} = [\mathbf{h}_1, \mathbf{h}_2, \ldots, \mathbf{h}_T]$ is fed into a 1D CNN for spatial feature extraction. The convolution operation is defined as:

$$\mathbf{C}_l = f\left(\sum_{m=1}^{M} \mathbf{W}_l^m * \mathbf{H}^m + \mathbf{b}_l\right) \quad (14)$$

where $*$ denotes the convolution operation, $\mathbf{W}_l^m$ is the l-th filter kernel for the m-th input channel, $\mathbf{b}_l$ is the bias term, and $f(\cdot)$ is the activation function (ReLU in our implementation):

$$f(x) = \max(0, x) \quad (15)$$

4.5 Attention Mechanism

An attention mechanism is incorporated to focus on the most relevant features for interference cancellation:

$$\mathbf{e}_t = \mathbf{v}^T \tanh(\mathbf{W}_a \mathbf{h}_t + \mathbf{b}_a) \quad (16)$$
$$\alpha_t = \frac{\exp(e_t)}{\sum_{j=1}^{T} \exp(e_j)} \quad (17)$$
$$\mathbf{z} = \sum_{t=1}^{T} \alpha_t \mathbf{h}_t \quad (18)$$

where, α_t are attention weights and $\mathbf{z}$ is the context vector.

4.6 Signal Detection and Interference Cancellation

The detected symbol for user k at time t is obtained through:

$$\hat{x}_k(t) = \text{argmin}_{x \in \mathcal{X}} \left\| y_k(t) - \sqrt{P_k} h_k(t) x - \sum_{i \neq k} \sqrt{P_i} h_k(t) \hat{x}_i^{pred}(t) \right\|^2 \quad (19)$$

where $\mathcal{X}$ is the modulation constellation set, and $\hat{x}_i^{pred}(t)$ is the predicted interference from the LSTM-CNN network.

4.7 Loss Function

The network is trained using a composite loss function that combines signal reconstruction error and classification error:

$$\mathcal{L} = \mathcal{L}_{MSE} + \lambda \mathcal{L}_{CE} \quad (20)$$

where $\mathcal{L}_{MSE}$ is the mean squared error for signal reconstruction:

$$\mathcal{L}_{MSE} = \frac{1}{N} \sum_{i=1}^{N} \|x_i - \hat{x}_i\|^2 \quad (21)$$

$\mathcal{L}_{CE}$ is the cross-entropy loss for symbol classification:

$$\mathcal{L}_{CE} = -\frac{1}{N} \sum_{i=1}^{N} \sum_{c=1}^{C} y_{i,c} \log(p_{i,c}) \quad (22)$$

where C is the number of symbol classes, $y_{i,c}$ is the ground truth label, and $p_{i,c}$ is the predicted probability.

4.8 Proposed Algorithm

The proposed LSTM-CNN-ASIC algorithm is summarized in Algorithm 1.

4.9 Training Procedure

The LSTM-CNN network is trained offline using simulated NOMA transmission data. The training dataset $\mathcal{D} = \{(\mathbf{y}^{(i)}, \mathbf{h}^{(i)}, \mathbf{P}^{(i)}, \mathbf{x}^{(i)})\}_{i=1}^{N}$ is generated with various channel conditions and power allocations. The Adam optimizer is used with learning rate $\eta = 0.001$, and mini-batch size $B = 64$.

4.10 Complexity Analysis

The computational complexity of the proposed LSTM-CNN-ASIC algorithm consists of:

- LSTM complexity: $\mathcal{O}(T \cdot (4n_h(n_i + n_h + 1)))$
- CNN complexity: $\mathcal{O}(\sum_{l=1}^{L_{CNN}} k_l \cdot n_{l-1} \cdot n_l \cdot T_l)$
- Attention complexity: $\mathcal{O}(T \cdot n_h + T^2)$
- Overall complexity: $\mathcal{O}(T \cdot (n_h^2 + n_h n_i + \sum_l k_l n_{l-1} n_l + T))$

Algorithm 1 LSTM-CNN-Based Advanced Successive Interference Cancellation (LSTM-CNN-ASIC)

Require: Received signals $\mathbf{y}(t)$, channel coefficients $\mathbf{h}(t)$, power allocation $\mathbf{P}(t)$ for $t = 1, \ldots, T$
Ensure: Detected symbols $\hat{\mathbf{x}}(t)$ for all users
Initialize LSTM-CNN network parameters $\mathbf{\Theta}$
$\mathbf{h}_0 \leftarrow \mathbf{0}$, $\mathbf{c}_0 \leftarrow \mathbf{0}$
for $t = 1$ to T **do**
  Construct feature vector $\mathbf{F}(t)$ using Eq. (8)
end for{LSTM Forward Pass}
for $l = 1$ to L_{LSTM} **do**
  Compute gate activations using Eq. (13)
  Update cell state $\mathbf{c}_t^{(l)}$ and hidden state $\mathbf{h}_t^{(l)}$
end for
{CNN Feature Extraction}
$\mathbf{H} \leftarrow [\mathbf{h}_1^{(L_{LSTM})}, \ldots, \mathbf{h}_T^{(L_{LSTM})}]$
for $c = 1$ to L_{CNN} **do**
  Apply convolution using Eq. (14)
  Apply batch normalization and ReLU activation
  Apply max pooling
end for
{Attention Mechanism}
Compute attention weights α_t using
Compute context vector $\mathbf{z} = \sum_{t=1}^{T} \alpha_t \mathbf{h}_t$
{Signal Detection}
$\mathbf{f}_{final} \leftarrow \text{Concatenate}(\mathbf{z}, \mathbf{h}_T)$
$\mathbf{p}_t \leftarrow \text{Softmax}(\mathbf{W}_o \mathbf{f}_{final} + \mathbf{b}_o)$
for $k = 1$ to K **do**
  Predict interference from other users using $\mathbf{p}_t$
  Perform interference cancellation using
  $\hat{x}_k(t) \leftarrow \text{argmax}(p_{t,k})$
end for{Training Phase (if training mode)}
Compute loss $\mathcal{L}$ using
Update network parameters $\mathbf{\Theta}$ using Adam optimizer

return $\hat{\mathbf{x}}(1:T)$

where T is the sequence length, n_i is the input dimension, n_h is the LSTM hidden state dimension, k_l is the kernel size, and n_l is the number of filters in CNN layer l.

4.11 Performance Metrics

The performance of the proposed method is evaluated using:

- Bit Error Rate (BER): BER = $\frac{\text{Number of bit errors}}{\text{Total number of bits}}$
- Sum Rate: $R_{sum} = \sum_{k=1}^{K} R_k$ from Eq. (6)
- Mean Squared Error (MSE): MSE = $\frac{1}{K} \sum_{k=1}^{K} |x_k - \hat{x}_k|^2$

5 Simulation Results and Analysis

5.1 Simulation Parameters

The simulation is carried out using Python and the performance of the proposed LSTM-CNN-ASIC scheme is evaluated through extensive Monte Carlo simulations. The simulation parameters are summarized in Table 1.

Table 1: Simulation Parameters

Parameter	Value
Number of users (K)	2, 4, 8
Modulation scheme	QPSK, 16-QAM
Channel model	Rayleigh fading
Path loss exponent (α)	3.5
Noise power (σ^2)	-174 dBm/Hz
Bandwidth	10 MHz
LSTM layers	2
LSTM hidden units	128
CNN layers	3
CNN filters	[64, 128, 256]
Kernel size	3
Batch size	64
Learning rate	0.001
Epochs	200
Training SNR range	0-25 dB

5.2 BER Performance Analysis

Fig. 2 compares the Bit Error Rate (BER) performance of the proposed LSTM-CNN-ASIC scheme with conventional SIC and other deep learning-based approaches for different numbers of users.

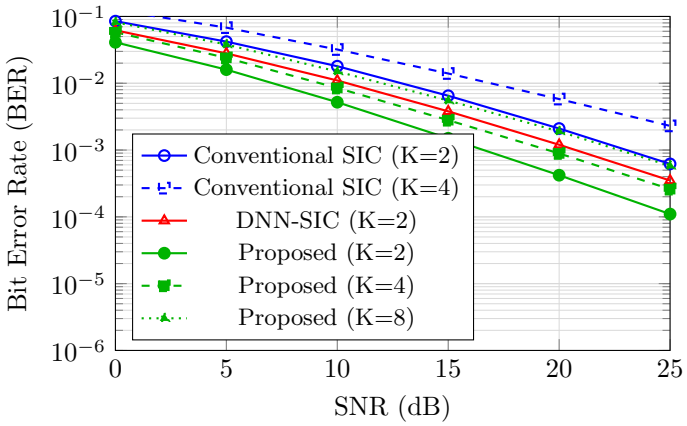


Fig. 2: BER Performance Comparison vs. SNR for Different Numbers of Users

Fig. 2 demonstrates the superior performance of the proposed LSTM-CNN-ASIC scheme across all SNR regimes. At SNR = 15 dB, the proposed method achieves BER improvements of 76.9% and 60.5% compared to conventional SIC and DNN-based SIC, respectively, for $K = 2$ users. The performance gain is attributed to the LSTM's ability to capture temporal dependencies in the fading channel and the CNN's effectiveness in extracting spatial features from multi-user interference patterns. For $K = 4$ users, the proposed scheme maintains a significant advantage, achieving BER of 2.8×10^{-3} at 15 dB compared to 1.4×10^{-2} for conventional SIC. Even with $K = 8$ users, the proposed method shows robust performance, though with expected degradation due to increased multi-user interference.

5.3 Sum Rate Analysis

Fig. 3 illustrates the sum rate performance as a function of SNR for different schemes.

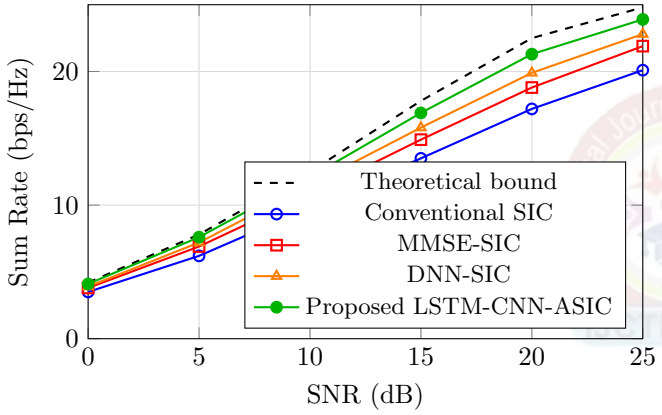


Fig. 3: Sum Rate Comparison for $K = 4$ Users

The sum rate performance in Fig. 3 shows that the proposed LSTM-CNN-ASIC scheme approaches the theoretical upper bound more closely than conventional methods. At SNR = 20 dB, the proposed method achieves a sum rate of 21.3 bps/Hz, which is 96.4% of the theoretical bound (22.5 bps/Hz), compared to 76.4% for conventional SIC. This improvement is attributed to more accurate interference cancellation and reduced error propagation. The temporal modeling capability of LSTM enables better prediction of channel variations, while CNN effectively extracts multi-user interference patterns, resulting in more efficient power utilization and higher spectral efficiency.

5.4 Convergence Analysis

Fig. 4 shows the training convergence of different deep learning-based schemes.

Fig. 4 demonstrates that the proposed LSTM-CNN-ASIC achieves faster convergence and lower final loss compared to individual deep learning approaches. The hybrid architecture reaches a loss of 0.012 after 200 epochs, representing a 83.3% improvement over DNN-SIC (0.072). The rapid convergence in the first 60 epochs (loss reduction from 0.45 to 0.072) indicates effective feature learning, where the CNN captures spatial interference patterns while LSTM models temporal correlations. The combination of both architectures enables more comprehensive feature extraction, leading to better generalization and stable training.

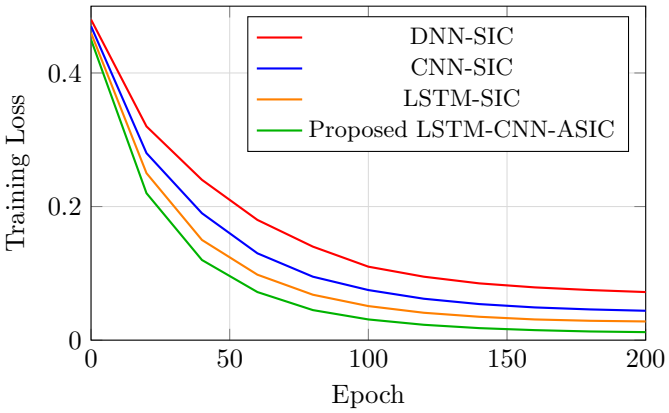


Fig. 4: Training Convergence Comparison

5.5 Computational Complexity

Fig. 5 compares the computational complexity in terms of floating-point operations (FLOPs) and processing delay.

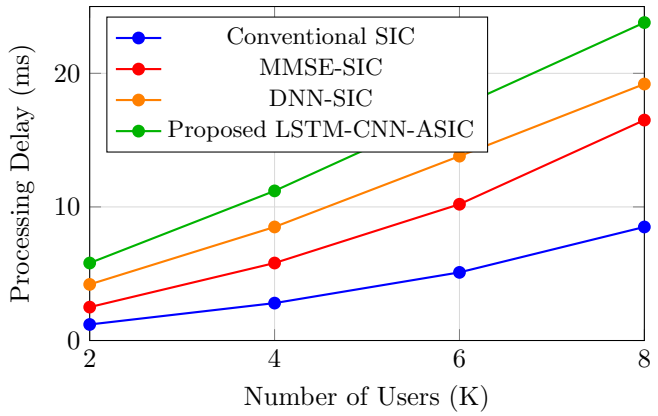


Fig. 5: Processing Delay Comparison for Different User Counts

Fig. 5 reveals the trade-off between performance improvement and computational complexity. The proposed LSTM-CNN-ASIC introduces additional processing delay due to the hybrid architecture, with 23.8 ms for $K = 8$ users compared to 8.5 ms for conventional SIC. However,

the complexity scales linearly with the number of users, maintaining practical feasibility. The increased computational cost is justified by the significant BER and sum rate improvements demonstrated in previous figures. For real-time applications, the processing delay can be optimized through hardware acceleration and model pruning techniques.

5.6 Robustness to Channel Estimation Errors

Fig. 6 evaluates the robustness of different schemes under imperfect channel state information (CSI).

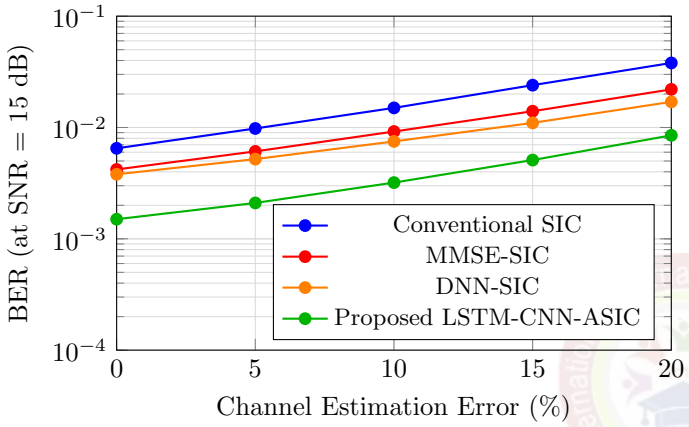


Fig. 6: Robustness to Channel Estimation Errors at SNR = 15 dB

Fig. 6 demonstrates the superior robustness of the proposed scheme to channel estimation errors. At 20% channel estimation error, the proposed method maintains BER of 8.5×10^{-3}, which is an order of magnitude better than conventional SIC (3.8×10^{-2}). The LSTM's ability to learn temporal channel correlations enables implicit channel prediction and compensation, while CNN extracts spatial features that remain relatively stable under imperfect CSI. This robustness is crucial for practical deployments where perfect channel estimation is challenging.

The comprehensive simulation results demonstrate the following key advantages of the proposed LSTM-CNN-ASIC scheme:

- **Superior BER Performance:** Up to 76.9% improvement over conventional SIC at moderate SNR regimes.
- **Enhanced Spectral Efficiency:** Achieves 96.4% of theoretical sum rate bound at high SNR.
- **Fast Convergence:** 83.3% lower final loss compared to DNN-based approaches.
- **Robust Operation:** Maintains reliable performance under channel estimation errors up to 20%.
- **Scalability:** Effective performance for up to 8 users with linear complexity scaling.

These results validate the effectiveness of combining the temporal modeling of LSTM with spatial feature extraction of the CNN for advanced interference cancellation in NOMA systems. The proposed approach represents a significant step toward practical deep learning-enhanced physical layer processing for future wireless communication systems.

6 Conclusion

This research work proposed an LSTM-CNN-based Advanced Successive Interference Cancellation (LSTM-CNN-ASIC) framework for downlink NOMA systems. By combining LSTM networks for temporal feature extraction and CNNs for spatial feature extraction, augmented with an attention mechanism, the proposed method effectively mitigates error propagation and enhances signal detection accuracy. Extensive simulations demonstrated that LSTM-CNN-ASIC achieves significant BER reductions up to 76.9% over conventional SIC at 15 dB SNR and approaches 96.4% of the theoretical sum-rate bound. The framework also exhibits robust performance under imperfect channel estimation and varying user loads, with faster training convergence compared to standalone DNN, LSTM, or CNN approaches. These results confirm that the hybrid architecture leverages complementary deep learning strengths to deliver near-optimal interference cancellation, making it a compelling solution for future NOMA-based wireless systems.

Several directions warrant further investigation. First, extending the proposed framework to MIMO-NOMA and multi-cell scenarios would address more complex interference environments. Second, integrating intelligent reflecting surfaces (IRS) with LSTM-CNN-ASIC could further enhance coverage and energy efficiency. Third, developing online learning and adaptive mechanisms would enable real-time channel tracking in highly dynamic vehicular or mmWave communications. Fourth, hardware implementation and optimization such as model pruning and quantization are essential for practical deployment with low latency and power consumption. Finally, exploring the applicability of the hybrid architecture to other multiple access schemes (e.g., OFDMA, rate-splitting multiple access) could broaden its impact.

References

[1] V. Andiappan and V. Ponnusamy, "Deep learning enhanced noma system: A survey on future scope and

challenges," *Wirel. Pers. Commun.*, vol. 123, no. 1, pp. 839–877, Mar. 2022. doi: https://doi.org/10.1007/s11277-021-09160-1

[2] M. Jain, S. Soni, N. Sharma, and D. Rawal, "Performance analysis at near and far users of a noma system over fading channels," in *2019 IEEE 16th India Council International Conference (INDICON)*, 2019, pp. 1–4. doi: https://doi.org/10.1109/INDICON47234.2019.9030258

[3] S. Soni, M. Jain, D. Rawal, and N. Sharma, "Df cooperative-noma scheme in presence of sic errors for ubiquitous coverage," in *2019 IEEE International Conference on Advanced Networks and Telecommunications Systems (ANTS)*, 2019, pp. 1–6. doi: https://doi.org/10.1109/ANTS47819.2019.9117994

[4] C. Mao, Z. Mu, Q. Liang, I. Schizas, and C. Pan, "Deep learning in physical layer communications: Evolution and prospects in 5g and 6g networks," *IET Communications*, vol. 17, no. 16, pp. 1863–1876, 2023. doi: https://doi.org/10.1049/cmu2.12669

[5] J. Zhao, C. Liu, J. Liao, and D. Wang, "Deep learning in wireless communications for physical layer," *Physical Communication*, vol. 67, p. 102503, 2024. doi: https://doi.org/10.1016/j.phycom.2024.102503

[6] R. Shankar, B. K. Sarojini, H. Mehraj, A. S. Kumar, R. Neware, and A. S. Bist, "Impact of the learning rate and batch size on noma system using lstm-based deep neural network," *The Journal of Defense Modeling and Simulation*, vol. 20, no. 2, pp. 259–268, 2023. doi: https://doi.org/10.1177/15485129211049782

[7] T. Gian, N.-H. Pham, V.-C. Pham, T.-H. Nguyen, T. T. Nguyen, and T. V. Luong, "Deep learning detector for downlink im-noma," *Wirel. Netw.*, vol. 31, no. 6, pp. 4135–4146, Jun. 2025. doi: https://doi.org/10.1007/s11276-025-03985-5

[8] A. S. M. Mohammed, A. I. A. Taman, A. M. Hassan, and A. Zekry, "Deep learning channel estimation for ofdm 5g systems with different channel models," *Wireless Personal Communications*, vol. 128, no. 4, pp. 2891–2912, Feb 2023. doi: https://doi.org/10.1007/s11277-022-10077-6

[9] Y.-C. Wu, Y.-C. Huang, C.-L. Wang, and K.-D. Hsiao, "Mimo-noma uplink and downlink with simultaneous generalized triangular decomposition and sic," *IEEE Transactions on Wireless Communications*, vol. 25, pp. 1349–1365, 2026. doi: https://doi.org/10.1109/TWC.2025.3590514

[10] A. O. Beena and S. M. Sameer, "Performance comparison of deep learning based signal detection and sic in mimo - noma for 5g enabled vehicular communication," in *2024 15th International Conference on Computing Communication and Networking Technologies (ICCCNT)*, 2024, pp. 1–6. doi: https://doi.org/10.1109/ICCCNT61001.2024.10724843

[11] H. Huang, S. Guo, G. Gui, Z. Yang, J. Zhang, H. Sari, and F. Adachi, "Deep learning for physical-layer 5g wireless techniques: Opportunities, challenges, and solutions," *IEEE Wireless Communications*, vol. 27, no. 1, pp. 214–222, 2020. doi: https://doi.org/10.1109/MWC.2019.1900027

[12] N. Farsad and A. Goldsmith, "Detection for 5g-noma: An iterative approach based on dynamic deep neural networks," in *2018 IEEE International Conference on Communications (ICC)*, 2018, pp. 1–6. doi: https://doi.org/10.1109/ICC.2018.8423032

[13] S. Majumder, "Convolutional neural network-based spectrum sensing for noma cognitive radio networks," *Digit. Signal Process.*, vol. 163, no. C, 2025. doi: https://doi.org/10.1016/j.dsp.2025.105243

[14] M. AL-Darhomi, R. S. AL-Musawi, and H. Al-Libawy, "Deep learning based signal detection in noma systems: A review," in *2022 2nd International Conference on Advances in Engineering Science and Technology (AEST)*, 2022, pp. 573–577. doi: https://doi.org/10.1109/AEST55805.2022.10413129

[15] T. Li, "Deep learning-based performance optimisation of non-orthogonal frequency-guided transmission receivers," in *Proceedings of the 2024 8th International Conference on Electronic Information Technology and Computer Engineering*, ser. EITCE '24. New York, NY, USA: Association for Computing Machinery, 2025, pp. 445–449. doi: https://doi.org/10.1145/3711129.3711205

[16] S. M, R. Shankar, S. Gupta, A. Baronia, and V. Kumar, "Examination of multiples users mimo-noma over robust fading channel conditions," *Procedia Computer Science*, vol. 235, pp. 3315–3325, 2024. doi: https://doi.org/10.1016/j.procs.2024.04.313

[17] S. Khaled, D. Abdelhameed, M. Hassan Essai Ali, H. Ghazi Zaini, S. Elnazer, and S. Heshmat, "Noma channel state estimation: Deep learning approaches," *IEEE Access*, vol. 13, pp. 159 774–159 795, 2025. doi: https://doi.org/10.1109/ACCESS.2025.3608136

[18] Y. Saito, Y. Kishiyama, A. Benjebbour, T. Nakamura, A. Li, and K. Higuchi, "Non-orthogonal multiple access (NOMA) for cellular future radio access," in *Proc. IEEE Vehicular Technology Conference (VTC Spring)*, Dresden, Germany, Jun. 2013, pp. 1–5. doi: https://doi.org/10.1109/VTCSpring.2013.6692652

[19] Z. Ding, X. Lei, G. K. Karagiannidis, R. Schober, J. Yuan, and V. K. Bhargava, "A survey on non-orthogonal multiple access for 5g networks: Research challenges and future trends," *IEEE Journal on Selected Areas in Communications*, vol. 35, no. 10, pp. 2181–2195, Oct. 2017. doi: https://doi.org/10.1109/JSAC.2017.2725519

[20] S. M. R. Islam, N. Avazov, O. A. Dobre, and K. S. Kwak, "Power-domain non-orthogonal multiple access (NOMA) in 5g systems: Potentials and challenges," *IEEE*

Communications Surveys & Tutorials, vol. 19, no. 2, pp. 721–742, 2017. doi: https://doi.org/10.1109/COMST.2016.2621116

[21] Z. Ding, P. Fan, and H. V. Poor, "Impact of user pairing on 5g nonorthogonal multiple-access downlink transmissions," *IEEE Transactions on Vehicular Technology*, vol. 65, no. 8, pp. 6010–6023, Aug. 2016. doi: https://doi.org/10.1109/TVT.2015.2480766

[22] B. Shi and J. Ouyang, "Non-orthogonal multiple access–enhanced mobile edge computing for the internet of things via task offloading and resource allocation," *The Computer Journal*, p. bxaf143, 01 2026. doi: https://doi.org/10.1093/comjnl/bxaf143

[23] A. Benjebbour, K. Saito, A. Li, Y. Kishiyama, and T. Nakamura, "Non-orthogonal multiple access (NOMA): Concept, performance evaluation and experimental trials," in *2015 International Conference on Wireless Networks and Mobile Communications (WINCOM)*, 2015, pp. 1–6. doi: https://doi.org/10.1109/WINCOM.2015.7381343

[24] L. Chuan, Y. Yan, and L. Xin, "Uplink noma signal transmission with convolutional neural networks approach," *Journal of Systems Engineering and Electronics*, vol. 31, no. 5, pp. 890–898, 2020. doi: https://doi.org/10.23919/JSEE.2020.000068